ACS Sustainable Chemistry & Engineering

Research Article

pubs.acs.org/journal/ascecg

Increasing Gas Hydrate Formation Temperature for Desalination of High Salinity Produced Water with Secondary Guests

Jong-Ho Cha and Yongkoo Seol*

National Energy Technology Laboratory, U.S. Department of Energy, Morgantown, West Virginia 26507, United States

Supporting Information

ABSTRACT: We suggest a new gas hydrate-based desalination process using water-immiscible hydrate formers; cyclopentane (CP) and cyclohexane (CH) as secondary hydrate guests to alleviate temperature requirements for hydrate formation. The hydrate formation reactions were carried out in an isobaric condition of 3.1 MPa to find the upper temperature limit of CO_2 hydrate formation. Simulated produced water (8.95 wt % salinity) mixed with the hydrate formers shows an increased upper temperature limit from −2 °C for simple CO_2 hydrate to 16 and 7 °C for double (CO_2 + CP) and (CO_2 + CH) hydrates, respectively. The resulting conversion rate to double hydrate turned out to be similar to that with simple CO_2 hydrate at the upper temperature limit. Hydrate formation rates (R_f) for the double hydrates with CP and CH are shown to be 22 and 16 times higher, respectively, than that of the simple CO_2 hydrate at the upper temperature limit. Such mild hydrate formation temperature and fast formation kinetics indicate increased energy efficiency of the double hydrate system for the desalination process. Dissociated water from the hydrates shows greater than 90% salt removal efficiency for the hydrates with the secondary guests, which is also improved from about 70% salt removal efficiency for the simple hydrates.

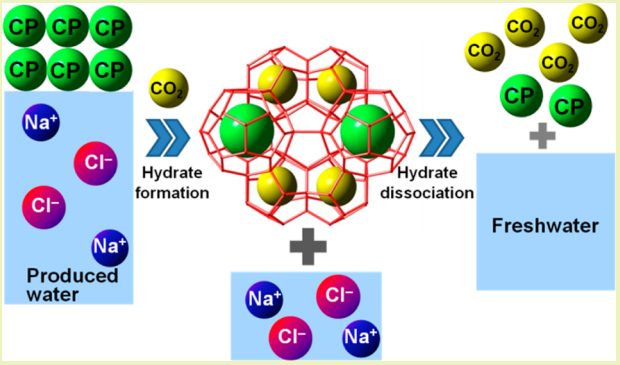

KEYWORDS: *Desalination, Gas hydrate, Produced water, Brine, Cyclopentane, Cyclohexane*

INTRODUCTION

Produced or flow back water is saline wastewater brought to the surface during gas and oil production or CO_2 sequestration operation in gas and oil fields.[1] The common constituents usually found in produced water include mineral ions; dispersed oil; dissolved hydrocarbons of alkane, aromatic compounds, and grease; heavy metals; radionuclides; and treatment chemicals for preventing operational problems.[2,3] The composition of produced water depends on the geologic characters of the reservoir formation, extraction methods, maturity of the oil field, and contact time with the oil in the formation. Typical concentrations of mineral ions range between 1% and 25%, and petroleum organics and suspended solids can be up to 0.15% and 0.1%, respectively.[2] Produced water is generally up to 9.5 times greater by volume than oil produced at oil fields in the United States.[1] The majority of produced water in offshore locations is discharged to the ocean.[4] More than 90% of the produced water generated in onshore locations is re-injected into wells for enhancing oil recovery or underground disposal sites that are deemed to be geologically isolated from underground sources of drinking water.[4] On the other hand, in water stressed regions, beneficial use of produced water such as irrigation, industrial uses, and recharge to water supplies has become an attractive option for produced water management. Thus, the treatment of produced water is an issue for safe reuse or discharge to the environment as produced water presents severe threats to crops and aquatic life.

Traditional treatments of produced water often include prior purification and desalination processes. Purification involves physical and chemical processes such as adsorption, filtration, reverse osmosis, coagulation, flocculation, and chemical oxidation for removal of suspended solid particles, heavy metals, and petroleum organics, and often requires a series of different treatment methods in order to achieve higher removal efficiency for various contaminants.[2] After those prior treatments, produced water can be desalinated by commercially well-established thermal distillation or reverse osmosis techniques.[5,6] Distillation is the oldest technique and most widely used worldwide, and freshwater is produced by water vapor condensate. The process, however, requires intensive energy use to provide heat for vaporization of feedwater and becomes very costly, especially when the operation of large capacity plants is involved. Therefore, most plants are located in the Middle East or North Africa where their petroleum resources can be used to offset limited water resources. Reverse osmosis, the most competing process against thermal distillation, uses semi-permeable membranes and pressure to

Received: September 28, 2012
Revised: July 9, 2013
Published: July 17, 2013

Table 1. Average Concentrations of Various Ions Presented in Produced Water

species	Ca^{2+}	Cl^-	Na^+	HCO_3^-	Mg^{2+}	SO_4^-	TDS	pH
avg.conc.(mg/L)	4874.56	53620.85	24609.11	656.05	1028.05	1131.56	89253.91	7.14

Table 2. Concentrations of Mineral Salts Used for Preparation of Synthetic Produced Water in This Study

species	NaCl	$CaCl_2$	$MgCl_2$	$CaCO_3$	Na_2SO_4	KCl	HCl	Total
conc. (g/L)	60.13	12.18	8.43	1.06	1.64	11.68	0.74	95.80
wt %	5.62	1.13	0.79	0.099	0.15	1.09	0.069	8.95

separate salts from water. This technique requires less energy than thermal distillation and has led to a reduction in overall desalination costs over the past decade. However, the short life times of membranes, pretreatment requirements for removal of impurities, and limits on operating pressure still remain as major hurdles of the reverse osmosis technique.

The gas hydrate desalination technique has been considered an alternative to conventional distillation and reverse osmosis techniques.[7−14] Because the chemical structure of gas hydrates includes only water and guest gaseous molecules, hydrate formation excludes all salts and other impurities from the crystalline structure leaving them in the residual saline water. When dissociated from the hydrate crystals, freshwater is recovered as a final product of the desalination process. The feasibility of seawater desalination via gas hydrate formation was already demonstrated during the 1960s.[12,13] In the mid 1990s, McCormack et al. conducted a pilot plant scale test for seawater desalination, which was sponsored by the Bureau of Reclamation in the United States.[11,14] The cost was estimated to be economically competitive to other desalination options. However, their estimations did not include the cost of seawater refrigeration that is required to bring the system into a hydrate stable condition as their process involves utilizing low temperature conditions in the deep seawater, and therefore, their test would not represent the feasibility of a typical land-based hydrate desalination process.

The recent needs of desalination for produced water containing up to 25% salinity and impurities from shale gas operations or the CO_2 sequestration process has renewed the interest in economic feasibility studies for the gas hydrate-based desalination process as other desalination processes show significantly limited efficiencies due to the severity of salinity in the produced water. Recently, it has been reported that the treatment by reverse osmosis facilities costs \$5.19−\$5.98/m^3,[15] which is quite higher than the seawater treatment cost of \$0.46−\$0.79/m^3 published elsewhere.[16] Such a large increment is mainly attributed to a decreased membrane lifetime due to increased operation pressures and pretreatment processes for removing contaminants. The distillation technique also shows energy consumption increases from 2.3 to 13.6 kWh/m^3 as salinity increases from 37 g/L for seawater to 55 g/L for produced water.[17,18] The gas hydrate-based desalination method will also be subjected to an increased operation cost due to higher pressure and lower temperature conditions for hydrate formation with the high salinity in produced water. However, hydrate formation conditions depend on guest species. In particular, introducing secondary organic guest substances can make the gas hydrate formation condition easily achievable, compared to simple CO_2 or CH_4 hydrate formation conditions, as they provide large stabilization energy to the hydrate framework.[19−21] Note that pressurized CO_2 stream from CO_2 emission sources may be easily available for hydrate formation, and the cost for pressurization is relatively low compared to that for refrigeration. Therefore, our search for a hydrate former has to be focused on those that can elevate the hydrate formation temperature, rather than alleviate the pressure requirement that has been suggested by using propane (C_3H_8) and hydrofluorocarbon (HFC) gases during past decades.[7,8,22]

Recently, Corak et al.[23] have suggested that the formation of simple cyclopentane (CP) hydrate could be used for seawater desalination. However, the hydrate system without gas guests was almost similar to the formation temperature for simple CO_2 hydrate. Herein, we suggest cyclopentane (CP) and cyclohexane (CH) hydrates formed with coguest CO_2 molecules at elevated temperature for the desalination of produced water with high salinity. CP and CH are known to form double structure-II (sII) hydrates with small gaseous molecules of CH_4 and CO_2. The larger $5^{12}6^4$ cages of the sII hydrates are occupied by CP and CH, and the smaller 5^{12} cages are filled with CH_4 or CO_2 molecules.[24−26] The formation temperature of double guest hydrate is shown to be higher than that of simple CP hydrate, as small cages are filled with CO_2 or CH_4 gaseous molecules. When compared to simple hydrates with single gaseous guest molecules, the phase boundary of double hydrates shifts into a hydrate promotion region represented by lower pressure and/or higher temperature.[26,27] Such a promotion effect is reported to be larger than that of THF, which is widely used as a hydrate promoter.[28] With more favorable hydrate formation conditions, CP hydrate has been suggested as the media for H_2 storage and CO_2 separation from pre- and postcombustion gases.[29−31] Additionally, the water immiscibility of CP and CH would be another advantage because it can allow the desalinated water to be easily separated from CP and CH.

This experimental study addressed an increase in hydrate formation kinetics, as well as an increase in hydrate formation temperature, when the hydrate formers are introduced in a hydrate-based desalination system. Salinity of water dissociated from the double hydrates was also examined to check the salt removal efficiency from the high salinity produced water. The main point of using the two hydrate formers would be thus to take advantage of their potential to elevate gas hydrate formation temperature and kinetics and subsequently to make the gas hydrate desalination process energy efficient, particularly for treating high salinity produced water.

EXPERMIENTAL SECTION

Materials. The chemicals used in this study were as follows. For synthesized produced water, we used NaCl (Sigma-Aldrich, > 99.0%), KCl (MP Biomedicals, > 99%), $CaCO_3$ (Fisher Scientific, > 99.0%), $CaCl_2$ (Acros Organics, 96%), $MgCl_2{\cdot}6H_2O$ (Acros Organics, > 99.0%), $NaSO_4$ anhydrous (Fisher Scientific, 99.3%), and HCl 1N solution (Sigma Aldrich). For hydrate formation, we used cyclo-

pentane (Sigma Aldrich, 99%), cyclohexane (Fisher Scientific, > 99%), and CO_2 gas (Airgas, 99.999%).

Composition of Produced Water. Representative salinity and composition of produced water was calculated based on the averaged data from 58,707 records in a preliminary database from oil and gas fields throughout 34 states provided by U.S. Geological Survey (USGS).[32] The averaged composition of produced water is listed in Table 1. On the basis of this information, we synthesized produced water using chemicals listed in Table 2. Organic constituents from in situ produced water were not included into the formulation of synthesized produced water because the study was focused on removal of mineral salts in the desalination process and detailed compositional data on the organics was not available.

Apparatus and Procedures for Hydrate Formation and Desalination. The hydrate formation reactor used in this study was a type 316 stainless steel round-bottomed cup with an internal volume of 120 cm^3, in which a magnetically driven mechanical stirrer was installed for mixing liquid sample. A stainless steel cap equipped with three access ports for gas input, output, and a thermocouple was placed on the reactor body. For temperature control, the body of the reactor was submersed in a pool of a water−ethylene glycol mixture, and the cap was enclosed with insulation material. Temperature and pressure in the reactor were measured by a K-type thermocouple (OMEGA) with a resolution of 0.1 K and a pressure transducer (Setra 205-2) with a digital readout (Setra Datum 2000), respectively.

For hydrate formation experiments, 35 g of synthesized produced water as control tests and 35 g produced water mixed with 7.30 g CP/8.77 g CH were used. The amounts of CP and CH correspond to the stoichiometric amount of 5.56 mol % for the 100% sII hydrate conversion from water, which could maximize the amount of hydrate formed from brine. The amount (35 g) of produced water was the minimum volume to allow the impeller to be submersed in the liquid phase, so that efficient and uniform mixing could be achieved for expedited hydrate formation kinetics. Prior to hydrate formation, the reactor was pressurized with CO_2 below expected equilibrium pressure at a designated temperature and slowly purged for 10 min at atmospheric pressure to remove air in the head volume. The purging was repeated three times. The hydrate formation reaction was initiated with pressurizing the reactor with CO_2 gas up to 3.1 MPa at various temperatures. During the test, the syringe pump (ISCO 260D) was operated at a constant pressure mode to keep the reactor pressure constant. As hydrate formation occurred, the volume in the syringe pump decreased, and the volume variation in the pump was recorded as a function of time every 30 s. Data acquisition and system operation were handled with LabView software (National Instruments). The experimental setup used in this study is described in Figure 1.

After the reaction was completed, hydrate removed from the reactor was crushed and filtered by vacuum suction (Fisher Scientific MaximaDry) for 4 min in order to remove the interstitial brine between hydrate crystals which lowers the desalination efficiency due to its high salt concentration. The harvested hydrate is dissociated at ambient condition, and water is separated from CP/CH by using their water immiscibility. The entire separation process to obtain desalinated water is schematically described in Figure 2.

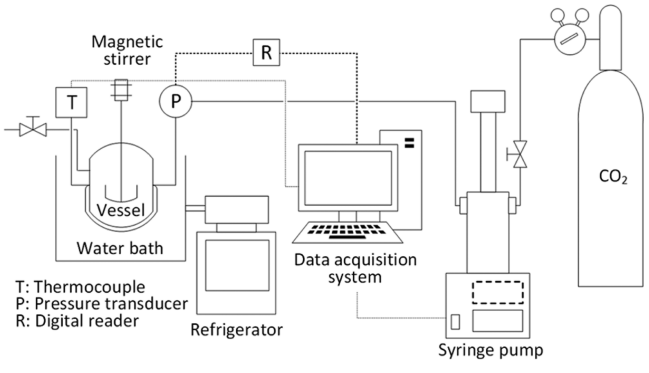

Figure 1. Experimental setup for hydrate formation reaction.

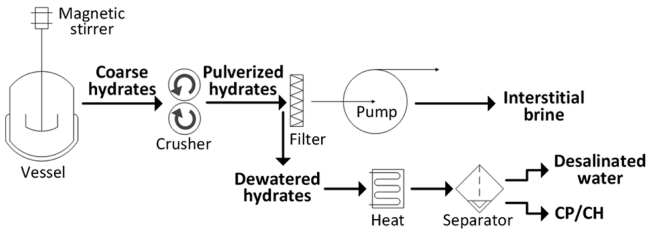

Figure 2. Schematic process of hydrate-based desalination technique using water-immiscible hydrate formers.

Hydrate Formation Kinetics. Hydrate formation kinetics was represented by CO_2 uptake as a function of time. At any given time, the total number of moles ($n_{T,t}$) in the closed system was kept constant and equal to that at time zero ($n_{T,0}$). Thus, the sum of the number of moles of gas in gas phase (n_G) and in hydrate phase (n_H) at any given time became the total number of moles in the reactor

$$n_{G,0} + n_{H,0} = n_{G,t} + n_{H,t}$$

The amount of CO_2 consumed was equal to that of CO_2 uptake in the hydrate phase

$$n_{H,t} - n_{H,0} = n_{G,0} - n_{G,t}$$

The variation of the internal volume in the syringe pump (V) was converted to the amount of consumed gas for hydrate formation as follow

$$\Delta n_H = n_{H,t} - n_{H,0} = n_{G,0} - n_{G,t} = \frac{P}{zRT}(V_0 - V_t)$$

where z was the compressibility factor calculated by Pitzer's correlation.[33]

Analysis of Ion Concentrations in Desalinated Water. The elemental analysis for cations dissolved in dissociated hydrate was performed using a Perkin-Elmer model Optima 3000 XL inductively coupled plasma atomic emission spectrometer (ICP-AES). Samples were introduced using a peristaltic pump at 1.0 mL/min in conjunction with an auto sampler. The resulting concentrations were used for calculating removal efficiency for each cation as follows

$$\text{Removal efficiency} = \frac{C_{A0} - C_A}{C_{A0}} \times 100$$

where C_{A0} and C_A were the concentration of each cation in the feed produced water and in dissociated hydrate crystals, respectively.

RESULTS AND DISCUSSION

CO_2 Hydrate Formation with Produced Water. The upper temperature limit of hydrate formation was confirmed for synthesized produced water with salinity of 8.95 wt % by CO_2 uptake profiles and visual observation of formed hydrate. Figure 3 shows CO_2 uptake profiles with three temperatures of −4.5, −2, and 0 °C at an isobaric condition of 3.1 MPa. The hydrate formation rates (R_f) were calculated from the initial slope showing a rapid increase in gas uptake in the profile. Both the R_f and total amount of CO_2 uptake were found to decrease with increasing temperature. Total CO_2 uptake at 0 °C was reduced to 5.4 mmol CO_2/mol H_2O, which corresponds to CO_2 solubility in the water solution and could not lead to hydrate formation. Whereas, the profiles at −4.5 and −2 °C present the CO_2 uptake enough to notice hydrate formation. Therefore, it was estimated in the present kinetic system that the upper temperature limit of hydrate formation is between −2 and 0 °C

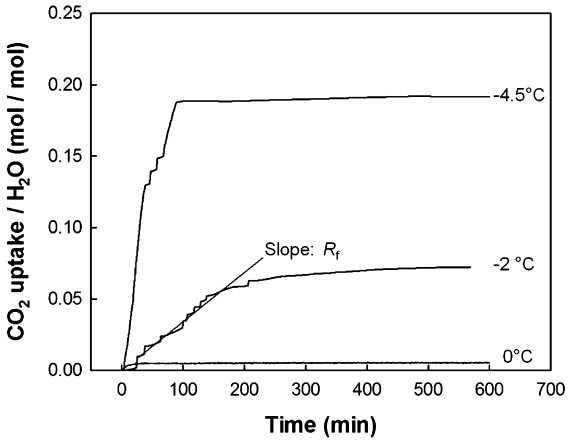

Figure 3. Profiles of CO_2 uptake in produced water with salinity of 8.95 wt % at −4.5, −2.0, and 0 °C. Operation pressure was 3.1 MPa.

at the salinity of 8.95 wt % and operation pressure of 3.1 MPa. The amount of CO_2 uptake and R_f are summarized in Table 3.

Table 3. Hydrate Formation Conditions, Total CO_2 Uptake in Hydrate Phase, Induction Time, and R_f for Each Sample at Isobaric Condition of 3.1 MPa

no.	guest	temperature (°C)	total CO_2 uptake (CO_2 mol/H_2O mol)	induction time[a] (min)	R_f (CO_2 mol/H_2O mol min^{-1})
1	CO_2	−4.5	0.192	0	3.74×10^{-3}
2	CO_2	−2.0	0.0723	23.5	3.44×10^{-4}
3	CO_2	0	0.00537	–	no hydrate
4	CO_2 + CP	7.0	0.0473	0	9.01×10^{-3}
5	CO_2 + CP	10.0	0.0387	0	8.19×10^{-3}
6	CO_2 + CP	13.0	0.0239	0	6.48×10^{-3}
7	CO_2 + CP	16.0	0.0234	0	7.48×10^{-3}
8	CO_2 + CH	2.5	0.123	0	1.019×10^{-2}
9	CO_2 + CH	4.0	0.0478	0	4.45×10^{-3}
10	CO_2 + CH	7.0	0.0262	0	5.67×10^{-3}
11	CO_2 + CH	9.0	0.00380	–	no hydrate

[a]Induction time was found by observing gas uptake time profiles and was assigned to the time period before rapid gas uptake resulting in growth of hydrate crystals.

The CO_2 hydrate formation reaction was duplicated at −2 °C for checking reproducibility. The hydrate nucleation is a stochastic process, and hydrate growth is known to be influenced by mass and heat transfer rates, implying that kinetics could vary even at pressure/temperature conditions with the same apparatus.[34] However, Figure S1 of the Supporting Information shows a R_f of 3.14×10^{-4} and 2.75×10^{-4} CO_2 mol/H_2O mol min^{-1} for each independent sample, which is quite close to that obtained from the profile at −2 °C in Figure 3.

The temperature-dependent hydrate formation shown in Figure 3 can be explained by the degree of subcooling, which is the difference between the experimental temperature and equilibrium temperature of the liquid water (L_w)−hydrate (H)−vapor (V) phase boundary at a given pressure and is represented by the driving force for simple hydrate formation.[35,36] Larger degrees of subcooling at low temperature therefore result in expedited kinetics and increased gas uptake for the hydrate formation as shown in Figure 3. When compared to the hydrate formation temperature of 6−7 °C at near 3.0 MPa for seawater,[9,37] the formation temperature for high salinity brine is substantially lower because the ion−dipole interaction between ionized mineral salts and water molecules becomes stronger than the hydrogen bonds between water molecules or the van der Waals forces for gas hydrate formation.[34] Such ion−water interaction makes the phase equilibrium boundary shift to the inhibition region represented by high pressure at a given temperature or low temperature at a given pressure. As a result, high salinity brine needs high pressure and low temperature for hydrate formation.

Hydrate Formation Promotion with Secondary Guests. Use of hydrate formers such as THF and tetraalkylammonium salts are reported to facilitate gas hydrate formation because the hydrate phase boundary is shifted to the promotion region with the formers.[19−21] Such promotion effects can be attributed to the large cage occupation of the hydrate formers. They provide sufficient stabilization energy for the clathrate framework even at near ambient pressure and, consequently, alleviate the temperature and pressure requirements for entrapment of gaseous molecules. On the basis of this inclusion behavior, we introduced CP into the produced water in an attempt to raise the hydrate formation temperature from subzero Celsius for the simple CO_2 hydrate to near ambient temperature.

Figure 4 displays the profiles of CO_2 uptake in the hydrate phase for double (CO_2 + CP) clathrate formation from the

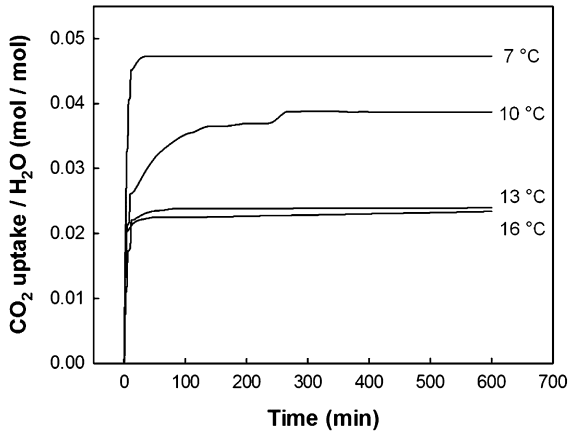

Figure 4. Profiles of CO_2 uptake in the mixture of produced water (salinity of 8.95 wt %) and CP at several temperatures and 3.1 MPa.

mixture of CP and produced water (8.95 wt % salinity). The hydrate formation profiles and visual observation of hydrate products confirm that the addition of CP raises the formation temperature of the double guest hydrate from −2 °C (for simple CO_2 hydrate) to 16 °C at 3.1 MPa. The result implies reduction of energy costs on refrigeration that accounts for a large portion of the total energy consumption in the hydrate formation process (Supporting Information). However, the amount of CO_2 uptake when the hydrate formation reaction was completed was lower than that of simple CO_2 hydrate, which can be explained by the occupation of CP in cages of the

hydrate phase. CO_2 molecules are known to form structure-I (sI) hydrates and fill small 5^{12} cages as well as large $5^{12}6^2$ cages.[38] A CSMGem software based on Gibbs energy minimization model predicts a small cage occupancy of 0.44−0.61 for the simple sI CO_2 hydrate in the temperature range of 2−9 °C at corresponding equilibrium pressure. Note that the occupancy approaches 0.6 as hydrate formation temperature increases. Thus, we assumed large $5^{12}6^2$ and small 5^{12} cage occupancies of 1.0 and 0.6 at near the upper temperature limit, respectively. A unit cell with 46 water molecules can situate 7.2 CO_2 molecules in six large cages and two small cages, giving a ratio of CO_2 to water of 0.157. In contrast, CP molecules would preferentially occupy the sII large $5^{12}6^4$ cages over the CO_2 molecules due to the better fitted size, whereas the remaining sII small 5^{12} cages are filled with CO_2 molecules as observed in other hydrate systems possessing 5^{12} cages.[39] Furthermore, the sII large cage occupation of hydrate formers results in lower sII small cage occupancy of gaseous molecules compared to sI small cage occupancy. The results obtained from CSMGem demonstrate that the sII double (C_3H_8 + CO_2) hydrate shows lower small cage occupancy of 0.27−0.46 for CO_2 molecules at the same temperature range with the above-mentioned simple CO_2 hydrate case. A similar tendency is also shown in sI simple CH_4 and sII double (CH_4 + THF) hydrate systems in the literature.[40] The sII hydrate consists of 8 large and 16 small cages in a unit cell with 136 water molecules. Thus, the CO_2-to-water ratio of 0.0588 can be obtained as it is conservatively assumed that small cage occupancy is 0.5 and eight CO_2 molecules are captured in a unit cell of sII hydrate. This simple calculation indicates that the amount of CO_2 uptake is reduced by formation of sII hydrate with double guests. The CO_2 uptake and cage occupancy assumed above demonstrates that the conversion rate to double hydrate at 16 °C is similar to that of the simple CO_2 hydrate at −2 °C (41% vs 46%, Supporting Information).

Recently, CP has been reported to improve the kinetics of gas hydrate formations in an emulsion system.[41] A similar tendency was also found in this work. The gas uptake profiles shown in Figure 4 present instantaneous hydrate formation (zero induction time) and increased R_f in the hydrate formation process. Repetition of the hydrate formation at 13 °C demonstrates good reproducibility for the kinetic behavior of a double guest system (Figure S2, Supporting Information). The R_f of 9.01×10^{-3} CO_2 mol/H_2O mol min^{-1} shown at 7 °C was 2.4 and 26 times higher than that for simple CO_2 hydrates at −4.5 and −2 °C, respectively (Table 3). Even though the higher R_f tended to decrease with temperature going up, it was almost retained until 16 °C, while the simple CO_2 hydrate system showed a sharply decreased R_f (Figure 5). Reduced R_f in the double guest system was observed above 16 °C after approximately 30 min from the beginning of hydrate formation as driving force decreases with temperature. Most of the hydrate formation reactions therefore reached full extent of CO_2 uptake within an hour in the case of the sII double hydrates formed at 16 °C or under, whereas simple CO_2 hydrate formation at −2 °C took a longer time due to its slower kinetics. A high R_f and resulting shorter time to complete hydrate reactions imply that more hydrate can be produced with a given time and reaction system.

The use of CH also raised the CO_2 hydrate formation temperature due to its inclusion in the sII large cages in a similar manner as with CP.[27] The kinetic profiles shown in Figure 6 and the visual examination of the hydrate formed

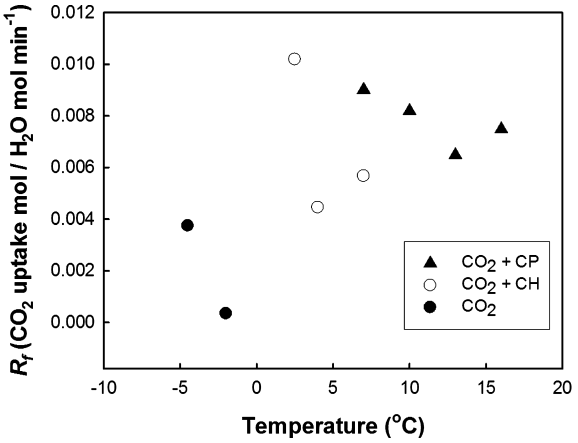

Figure 5. R_f calculated from slopes of each profiles for the formation of simple CO_2 and double (CO_2 + CP) and (CO_2 + CH) hydrates at varying temperatures.

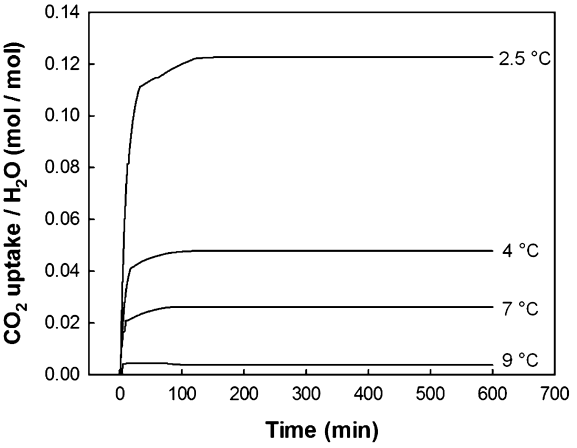

Figure 6. Profiles of CO_2 uptake in the mixture of produced water (salinity of 8.95 wt %) and CH at several temperatures and 3.1 MPa.

demonstrate that the formation temperature is elevated up to 7 °C at 3.1 MPa. The resulting R_f for the double (CO_2 + CH) hydrate at 7 °C was found to be 16 times higher than that of the simple CO_2 hydrate at −2 °C (Figure 5 and Table 3). Thus, both the upper temperature limit and R_f for hydrate formation become more favorable for energy efficient hydrate formation in the order of double (CO_2 + CP), double (CO_2 + CH), and simple CO_2 hydrates.

In general, hydrate formers alleviate the high pressure and low temperature requirements for gas hydrate formation. It is reported that CP is well-fitted into sII large cages to form simple sII CP hydrate without any gaseous guests (so-called *"help gas"*) to aid in the hydrate formation of large guest species that cannot be enclathrated by itself, and additional small cage occupation by gas molecules results in a more stabilized hydrate framework.[24,42,43] On the contrary, CH has to accompany small gaseous molecules filling sII small cages in order to form sII CH hydrates due to its insufficient stabilization energy.[24] Recent model computation using the DLpoly2 package indicates that interaction energy between CP and host cages is more negative than that between CH and cages (−40 vs −26 kJ mol^{-1}).[44] Thus, the more negative energy of CP, which means a larger stabilization energy, can result in a phase boundary curve for double (CO_2 + CP) hydrate shifted into the high temperature and low pressure region and having CO_2 enclathrated in sII

small cages at a milder condition, compared to a double (CO_2 + CH) guest system.[27] However, the double CH hydrate formed with *"help gas"* CO_2 providing auxiliary stabilization energy still presents the promotion effect and thus requires a milder condition for hydrate formation compared to the simple CO_2 hydrate.

Removal of Mineral Salts by Hydrate Formation. During the hydrate formation process, brine solution becomes concentrated as salts are excluded from the hydrate structures. The high salinity residual water would then be trapped between hydrate crystals. The interstitial water causes significant salinity in the water when dissociated from hydrate and requires additional repetitive steps of the hydrate formation process to achieve an acceptable level of salinity.[45] Thus, the development of a technique to efficiently separate the residual interstitial brine from the hydrate crystal has been another challenging issue. In the present work, hydrate harvested from the reactor was crushed and filtered by vacuum suction for removing the interstitial water. Figure 7 shows removal efficiency of various

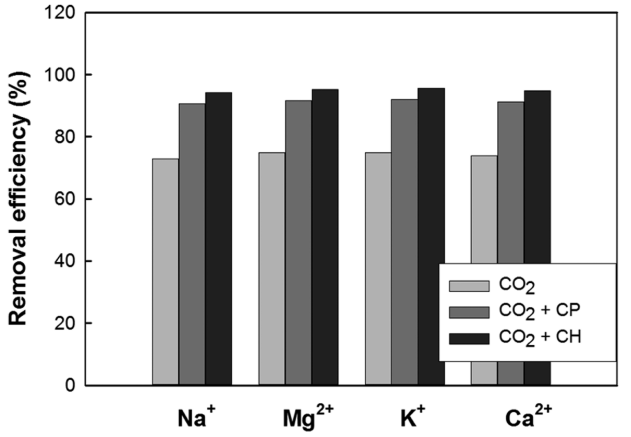

Figure 7. Removal efficiency (%) of each cation dissolved in the desalinated water.

cations from the simulated produced water. It was found that the efficiencies for each cation were almost the same in all the hydrate crystals collected after filtration and reached about 74%, 91%, and 95% for simple CO_2 (sample 2), double (CO_2 + CP) (sample 5), and double (CO_2 + CH) hydrates (sample 9), respectively.

After the hydrate was harvested and dissociated at ambient pressure, CP and CH can be separated from water phase using their water immiscibility and can be recycled and reused for the next hydrate reaction batches. However, the solubilities of CP and CH are reported to be 86 and 67 mg/L at 10 °C, respectively,[46] and the corresponding amount of hydrate promoters would still be dissolved in the water phase. It should be noted that commercial produced water treatment systems are typically equipped with facilities in pre-treatment or post-treatment mode capable of removing petroleum organics and suspended solids. The treatment facilities can also be used for removal of a smaller amount of CP or CH dissolved in the water if desalinated water requires a high water quality standard.

In the present work, we suggested the use of two water-immiscible hydrate formers for making CO_2 hydrate formation occurring at near ambient temperature. Inclusions of CP and CH in the hydrate phase present an increased R_f at high temperature as well as the lifted upper temperature limit of hydrate formations from −2 °C for the simple CO_2 hydrate system to nearly ambient temperature at 16 and 7 °C, respectively. The results indicate that this approach employing the hydrate formers enhances the hydrate formation process in terms of energy consumption and reaction time. On the basis of these laboratory scale results, larger scale studies need to be carried out to further verify the economics of the double hydrate desalination system over other traditional desalination methods.

■ ASSOCIATED CONTENT

Supporting Information

Additional profiles of CO_2 uptake for independent runs of simple CO_2 and double (CO_2 + CP) hydrate formations for checking reproducibility of kinetic behaviors. Refrigeration energies required to bring simple CO_2 and double (CO_2 + CP) hydrates into the hydrate formation region from room temperature and calculation of hydrate conversion rate from CO_2 uptake profiles. This material is available free of charge via the Internet at http://pubs.acs.org.

■ AUTHOR INFORMATION

Corresponding Author

*E-mail: Yongkoo.Seol@netl.doe.gov. Tel.: 1-304-285-2029.

Notes

The authors declare no competing financial interest.

■ ACKNOWLEDGMENTS

The authors thank the National Energy Technology Laboratory for financial support. The authors also thank Jinesh Jain for assistance of analysis on cation concentrations and Wu Zhang and Prof. Ki-Sub Kim for valuable comments for improving the paper.

■ ABBREVIATIONS

CP, cyclopentane; CH, cyclohexane; sI, structure I; sII, structure II; R_f, hydrate formation rate

■ REFERENCES

(1) Viel, J. A.; Puder, M. G.; Elcock, D.; Redweik, R. J., Jr. *A White Paper Describing Produced Water from Production of Crude Oil, Natural Gas, and Coal Bed Methane*; Argonne National Laboratory: Argonne, IL, 2004. http://www.ipd.anl.gov/anlpubs/2004/02/49109.pdf.

(2) Ahmadun, F.-R.; Pendashteh, A.; Abdullah, L. C.; Biak, D. R. A.; Madaeni, S. S.; Abidin, Z. Z. Review of technologies for oil and gas produced water treatment. *J. Hazard. Mater.* **2009**, *170*, 530−551.

(3) Tellez, G. T.; Nirmalakhandan, N.; Gardea-Torresdey, J. L. Kinetic evaluation of a field-scale activated sludge system for removing petroleum hydrocarbons from oilfield-produced water. *Environ. Prog.* **2005**, *24*, 96−104.

(4) Clark, C. E.; Veil, J. A. *Produced Water Volumes and Management Practice in the United States*; Argonne National Laboratory: Argonne, IL, 2009. http://www.netl.doe.gov/technologies/coalpower/ewr/water/pdfs/anl%20produced%20water%20volumes%20sep09.pdf

(5) Khawaji, A. D.; Kutubkhanah, I. K.; Wie, J.-M. Advances in seawater desalination technologies. *Desalination* **2008**, *221*, 47−69.

(6) Cipollina, A., Micale, G., Rizzuti, L., Eds. *Seawater Desalination: Conventional and Renewable Energy Processes*; Springer: Heidelberg, Germany, 2009.

(7) Sugi, J.; Saito, S. Concentration and demineralization of sea water by the hydrate process. *Desalination* **1967**, *3*, 27−31.

(8) Kubota, H.; Shimizu, K.; Tanaka, Y.; Makita, T. Thermodynamic properties of R13 ($CCIF_3$), R23 (CHF_3), R152a ($C_2H_4F_2$), and

propane hydrates for desalination of sea water. *J. Chem. Eng. Jpn.* **1984**, *17*, 423−429.
(9) Park, K.-n.; Hong, S. Y.; Lee, J. W.; Kang, K. C.; Lee, Y. C.; Ha, M.-G.; Lee, J. D. A new apparatus for seawater desalination by gas hydrate process and removal characteristics of dissolved minerals (Na^+, Mg^{2+}, Ca^{2+}, K^+, B^{3+}). *Desalination* **2011**, *274*, 91−96.
(10) Ngan, Y. T.; Englezos, P. Concentration of mechanical pulp mill effluents and NaCl solutions through propane hydrate formation. *Ind. Eng. Chem. Res.* **1996**, *35*, 1894−1900.
(11) McCormack, R. A.; Anderson, R. K. *Clathrate Desalination Plant: Preliminary Research Study*; Water Treatment Technology Program Report No. 5; Thermal Energy Storage, Inc.: San Diege, CA, 1995. http://www.usbr.gov/pmts/water/publications/reportpdfs/report005.pdf.
(12) Barduhn, A. J.; Towlson, H. E.; Hu, Y. C. The properties of some new gas hydrates and their use in demineralizing sea water. *AIChE J.* **1962**, *8*, 176−183.
(13) Barduhn, A. J. Desalination by crystallization processes. *Chem. Eng. Prog.* **1967**, *63*, 98−103.
(14) McCormack, R. A.; Niblock, G. A. *Build and Operate a Clathrate Desalination Pilot Plant*; Water Treatment Technology Program Report No. 31; Thermal Energy Storage, Inc.: San Diege, CA, 1998. http://www.usbr.gov/pmts/water/publications/reportpdfs/report031.pdf.
(15) Çakmakcı, M.; Kayaalp, N.; Koyuncu, I. Desalination of produced water from oil production fields by membrane processes. *Desalination* **2008**, *222*, 176−186.
(16) El-Dessouky, H. T. Ettouney, H. M. *Fundamentals of Salt Water Desalination*; Elsevier Science: Amsterdam, The Netherlands, 2002.
(17) Wade, N. M. Distillation plant development and cost update. *Desalination* **2001**, *136*, 3−12.
(18) Koren, A.; Nadav, N. Mechanical vapour compression to treat oil field produced water. *Desalination* **1994**, *98*, 41−48.
(19) Kang, S.-P.; Lee, H. Recovery of CO_2 from flue gas using gas hydrate: Thermodynamic verification through phase equilibrium measurements. *Environ. Sci. Technol.* **2000**, *34*, 4397−4400.
(20) Lee, H.; Lee, J.-w.; Kim, D. Y.; Park, J.; Seo, Y.-T.; Zeng, H.; Moudrakovski, I. L.; Ratcliffe, C. I.; Ripmeester, J. A. Tuning clathrate hydrates for hydrogen storage. *Nature* **2005**, *434*, 743−746.
(21) Arjmandi, M.; Chapoy, A.; Tohidi, B. Equilibrium data of hydrogen, methane, nitrogen, carbon dioxide, and natural gas in semi-clathrate hydrates of tetrabutyl ammonium bromide. *J. Chem. Eng. Data* **2007**, *52*, 2153−2158.
(22) Englezos, P. Clathrate hydrates. *Ind. Eng. Chem. Res.* **1993**, *32*, 1251−1274.
(23) Corak, D.; Barth, T.; Høiland, S.; Skodvin, T.; Larsen, R.; Skjetne, T. Effect of subcooling and amount of hydrate former on formation of cyclopentane hydrates in brine. *Desalination* **2011**, *278*, 268−274.
(24) Ripmeester, J. A.; Ratcliffe, C. I.; McLaurin, G. E. The Role of Heavier Hydrocarbons in Hydrate Formation. AIChE Spring Meeting, Session 44, *Hydrates in the Gas Industry*, **1991**.
(25) Mooijer-van den Heuvel, M. M.; Witteman, R.; Peter, C. J. Phase behaviour of gas hydrates of carbon dioxide in the presence of tetrahydropyran, cyclobutanone, cyclohexane and methylcyclohexane. *Fluid Phase Equilib.* **2001**, *182*, 97−110.
(26) Sun, Z.-G.; Fan, S.-S.; Guo, K.-H.; Shi, L.; Cuo, Y.-K.; Wang, R. Z. Gas hydrate phase equilibrium data of cyclohexane and cyclopentane. *J. Chem. Eng. Data* **2002**, *47*, 313−315.
(27) Mohammadi, A. H.; Richon, D. Phase equilibria of clathrate hydrates of methyl cyclopentane, methyl cyclohexane, cyclopentane or cyclohexane + carbon dioxide. *Chem. Eng. Sci.* **2009**, *64*, 5319−5322.
(28) Komatsu, H.; Yoshioka, H.; Ota, M.; Sato, Y.; Watanabe, M.; Smith, R. L., Jr; Peters, C. J. Phase equilibrium measurements of hydrogen−tetrahydrofuran and hydrogen−cyclopentane binary clathrate hydrate systems. *J. Chem. Eng. Data* **2010**, *55*, 2214−2218.
(29) Trueba, A. T.; Rovetto, L. J.; Florusse, L. J.; Kroon, M. C.; Peters, C. J. Phase equilibrium measurements of structure II clathrate hydrates of hydrogen with various promoters. *Fluid Phase Equilib.* **2011**, *307*, 6−10.
(30) Zhang, J.; Yedlapalli, P.; Lee, J. W. Thermodynamic analysis of hydrate-based pre-combustion capture of CO_2. *Chem. Eng. Sci.* **2009**, *64*, 4732−4736.
(31) Li, S.; Fan, S.; Wang, J.; Lang, X.; Wang, Y. Clathrate hydrate capture of CO_2 from simulated flue gas with cyclopentane/water emulsion. *Chinese J. Chem. Eng.* **2010**, *18*, 202−206.
(32) Breit, G. USGS Produced Water Database; U.S. Geological Survey: Denver, CO, 2002. http://energy.cr.usgs.gov/prov/prodwat/data.htm.
(33) Smith, J. M., Van Ness, H., Abbott, M. *Introduction to Chemical Engineering Thermodynamics*, 7th ed.; McGraw Hill: New York, 2005.
(34) Sloan, E. D., Koh, C. A. *Clathrate Hydrates of Natural Gases*, 3rd. ed.; CRC Press: Boca Raton, FL, 2008.
(35) Vysniauskas, A.; Bishnoi, P. R. A kinetic study of methane hydrate formation. *Chem. Eng. Sci.* **1983**, *38*, 1061−1072.
(36) Arjmandi, M.; Tohidi, B.; Danesh, A.; Todd, A. C. Is subcooling the right driving force for testing low-dosage hydrate inhibitors? *Chem. Eng. Sci.* **2005**, *60*, 1313−1321.
(37) Ohgaki, K.; Makihara, Y.; Takano, K. Formation of CO_2 hydrate in pure and sea water. *J. Chem. Eng. Jpn.* **1993**, *26*, 558−564.
(38) Udachin, K. A.; Ratcliffe, C. I.; Ripmeester, J. A. Structure, composition, and thermal expansion of CO_2 hydrate from single crystal X-ray diffraction measurements. *J. Phys. Chem. B* **2001**, *105*, 4200−4204.
(39) Shin, H. J.; Lee, Y.-J.; Im, J.-H.; Han, K. W.; Lee, J.-W.; Lee, Y.; Lee, J. D.; Jang, W.-Y.; Yoon, J.-H. Thermodynamic stability, spectroscopic identification and cage occupation of binary CO_2 clathrate hydrates. *Chem. Eng. Sci.* **2009**, *64*, 5125−5130.
(40) Seo, Y.-T.; Lee, H. ^{13}C NMR analysis and gas uptake measurements of pure and mixed gas hydrates: Development of natural gas transport and storage method using gas hydrate. *Korean J. Chem. Eng.* **2003**, *20*, 1085−1091.
(41) Galfré, A.; Fezoua, A.; Ouabbas, Y.; Cameirao, A.; Herri, J. M. Carbon Dioxide Hydrates Crystallization in Emulsion, 7th International Conference on Gas Hydrate (ICGH 2011), Edinburgh, U.K.
(42) Nakajima, M.; Ohmura, R.; Mori, Y. H. Clathrate hydrate formation from cyclopentane-in-water emulsions. *Ind. Eng. Chem. Res.* **2008**, *47*, 8933−8939.
(43) Zhang, Y.; Debenedetti, P. G.; Prud'homme, R. K.; Pethica, B. A. Differential scanning calorimetry studies of clathrate hydrate formation. *J. Phys. Chem. B* **2004**, *108*, 16717−16722.
(44) Frankcombe, T. J.; Kroes, G.-J. A new method for screening potential sII and sH hydrogen clathrate hydrate promoters with model potentials. *Phys. Chem. Chem. Phys.* **2011**, *13*, 13410−13420.
(45) Bradshaw, R. W.; Greathouse, J. A.; Cygan, R. T.; Simmons, B. A.; Dedrick, D. E.; Majzoub, E. H. *Desalination Utilizing Clathrate Hydrates*; LDRD Final Report; Sandia National Laboratories: Albuquerque, NM, Livermore, CA, 2008. http://prod.sandia.gov/techlib/access-control.cgi/2007/076565.pdf.
(46) Énglin, B. A.; Platé, A. F.; Tugolukov, V. M.; Pryanishnikova, M. A. Service properties of fuels and oils. *Chem. Tech. Fuels Oil* **1965**, *1*, 722−726.